

Subsidence in Guayanilla: Challenges in the Southern Zone of Puerto Rico

Valeria A. Pérez Rivera¹, Sharlyn N. Agosto Reyes²

^{1,2}Geology Department, University of Puerto Rico, Mayagüez Campus

Abstract

The study investigates subsidence and alterations in coastal wetlands from 2019 to 2024 in Punta Ventana Beach and the El Faro community in Guayanilla, Puerto Rico, following a seismic sequence that commenced on December 28, 2019. Analysis utilized Sentinel-1A and Landsat 8 OLI/TIRS imagery to assess subsidence patterns. Sentinel-1A data was processed in SNAP, while Landsat 8 OLI/TIRS imagery was processed in ENVI 6 for enhanced accuracy. Results indicate subsidence of 0.058 m in the El Faro community and 0.082 m in Punta Ventana Beach. Subsidence in both areas led to coastal inundation, observed through NDVI calculations in ENVI and aerial images from Google Earth. This escalation in vulnerability exacerbates the risks faced by the El Faro coastal community amidst atmospheric events, storm tides, and potential tsunami events.

Keywords: earthquake, inundation, subsidence, Guayanilla

I. Introduction

Coastal regions represent dynamic interfaces where land meets the ocean, undergoing constant evolution shaped by various processes, sedimentation patterns, and underlying geological compositions. In Puerto Rico, these coastal landscapes typically feature limestone and sandstone rock formations, contributing to the presence of carbonate sand in these areas. The coastal zones of Puerto Rico encompass a diverse range, including

sandy shores, rocky cliffs, mangrove-dominated coastlines with a presence of clay and silt grain size sediment, and alluvial areas (Barreto, 2017). With 44 coastal municipalities and a remarkable 1,225 beaches, Puerto Rico's coastline constitutes a significant portion of its geography, comprising approximately 30% of the island's total coastal area (Barreto, M. et al., 2019). These coastal areas are integral to Puerto

Rico's tourism and economy, underscoring their importance in driving the island's prosperity and cultural identity.

Coastal regions worldwide face inherent vulnerability to seismic hazards such as earthquakes and tsunamis. Puerto Rico, situated within a geologically active zone since the XVII century, is particularly prone to seismic activity. Due to the prevalence of soft and loose sedimentary soils in these areas, seismic events can induce significant vertical movements along the coastline. For instance, during earthquakes, liquefaction of sandy substrates may trigger sudden subsidence, resulting in the sinking of coastal land. This subsidence, coupled with the impact of sea-level rise, exacerbates the risk of flooding, posing substantial threats to coastal infrastructure and communities' integrity and resilience (Styron, 2019).

The gradual subsidence of coastal land and persistent inundation can contribute to the emergence of barrier islands and islets. These dynamic formations serve as habitat for diverse wildlife, flora, and human communities. Often aligned in chains along coastlines, barrier islands and islets are delineated by narrow tidal inlets and are typically separated from the mainland by shallow water, bays, or lagoons (NOAA, 2021). Tectonic movements, such as subsidence or uplift, also play a significant role in their formation. Subsidence causes portions of land to sink below sea level, leading to the creation of isolated land masses, while uplift exposes previously submerged areas, resulting in the formation of new islets.

Understanding coastal subsidence, a critical phenomenon with significant implications for coastal communities,

requires employing various techniques. Both space-borne and land-based approaches are utilized for studying this phenomenon. Space-borne techniques involve satellites equipped with synthetic aperture radar (SAR) to monitor changes in land elevation over time. On the other hand, land-based techniques utilize ground-based instruments like tide gauges, providing localized measurements at specific coastal locations (Shirzaei et al., 2021).

Among the satellites utilized for observing coastal changes are Sentinel-1A and Landsat 8-OLI/TIRS. The former, renowned for its adeptness in monitoring terrestrial surfaces for motion-related risks such as subsidence and landslides, boasts a temporal resolution of 12 days (Sentinel-1, copernicus.eu). Additionally, it offers diverse acquisition modes tailored to varying spatial coverage needs. OLI presents an opportunity to scrutinize coastal surface areas with a spatial resolution of 30 m, with a panchromatic band of 15 m. Operating at a temporal resolution of 16 days, OLI contributes to the comprehensive understanding of coastal dynamics (Landsat 8, usgs.gov).

Integration of data from satellites such as Sentinel-1A and Landsat 8-OLI/TIRS underscores a holistic approach to comprehending coastal subsidence and changes processes.

1.1 Study Site

Located in the northeastern corner of the Caribbean Plate, Puerto Rico intersects with the North American Plate (**Figure 1**), rendering it a region of significant geological activity. In 2020, the island witnessed a series of seismic events, characterized by fault ruptures and

moderate-magnitude earthquakes, notably within the Southwest Puerto Rico earthquake sequence. Among these occurrences, the most notable was a Mw6.4 seismic event originating approximately 15 km southeast of Indios, at a depth of 8.6 km, along a relatively small offshore fault. This fault, adjacent to the Punta Montalva fault, exhibits a northeast-striking, southwest-dipping normal fault orientation.

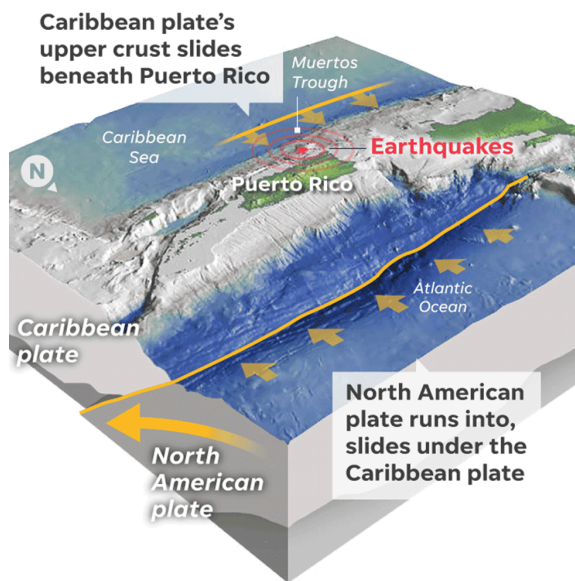


Figure 1: Tectonic setting of Puerto Rico. The island is being squeezed by the two tectonic plates, the North American and Caribbean Plates. Source: U.S. Geological Survey, NOAA Ocean Exploration and Research.

The aftermath of these seismic activities, particularly the Mw6.4 earthquake, resulted in substantial damage to coastal towns, with Guayanilla bearing a significant brunt. Particularly impacted was the community of El Faro coastal environment, which, historically, had only experienced water influx during high tides or storms. However, following the Mw6.4 earthquake, the intertidal lagoon within

this community suffered ocean intrusion, leading to persistent flooding. Similarly, Punta Ventana Beach, distinguished by its cliff resembling a window, experienced a collapse during the Mw6.4 earthquake. Nestled between cliffs and swamps, this hidden beach holds a unique charm in Puerto Rico. Over time, the coastal environment has undergone dramatic changes, notably with increased flooding in the swampy areas.

Recognizing the need to investigate potential coastline deformation post-2020 seismic activity, efforts were initiated to conduct a thorough examination of Guayanilla's coastal landscape.

1.2 Objectives

The primary aim of this study was to assess the impact of the seismic sequence in southern Puerto Rico on the coastal environments of Guayanilla. Focusing on the coastal areas of Guayanilla, our hypothesis posited that annual changes occur within these environments, including variations in elevation over the study period. The specific objectives are as follows:

- 1) Observe if southern subsidence has increased over the years (2020-2023).
- 2) Understand what changes in coastal environments occurred through two locations in Guayanilla (2019-2024).
- 3) Observe elevation changes from 2019 compared to current elevation in 2023.
- 4) With all the above, understand what could affect the population living in the community of El Faro places.

The question that will be answer:
Does seismic activity continue to affect the level of the coastal environment in the south of the island, especially in Guayanilla?

II. Methodology

2.1: Subsidence Maps

For the generation of subsidence maps, Level-1 satellite images from the Synthetic Aperture Radar C-band (C-SAR) instrument onboard the Sentinel-1A satellite were utilized. These images were acquired from the Copernicus Data Space Ecosystem website of the European Space Agency (ESA). For the purpose of the study, a total of four images were obtained spanning two distinct time intervals: one from July 8th to 20th, 2019, and the other from July 11th to 30th, 2023.

Upon accessing the Sentinel Platform, known as SNAP, the following steps, comprising multiple substeps, were executed to process the images: (1) TOPSAR split with a vertical-vertical (VV) polarisation; (2) InSAR processing; (3) DInSAR processing; (4) Phase Unwrapping; and, (5) Displacement Map.

The InSAR processing encompassed several distinct substeps, including: Read the split files, Apply-Orbit File, Back-Geocoding, Enhanced Spectral Diversity, Interferogram, TOPSAR-Deburst, and Write. This processing step aims to derive the phase difference between the two images, capturing both topographical features and deformation patterns.

The DInSAR processing comprised the subsequent steps: Read, TopoPhaseRemoval, Goldstein Phase/Filtering, Snaphu Export, and Write. This process yielded a differential interferogram exclusively depicting ground deformation.

The Phase Unwrapping procedure involved the execution of the following steps: Read, Snaphu Import, Phase-to-Displacement, Range Doppler Correction, and Write. This phase provided displacement measurements, facilitating the generation of georeferenced displacement maps. Subsequently, these maps were saved in ENVI format and imported into the ENVI platform. The maps were then cropped using the Resize Raster tool. To enhance visual interpretation, a color palette, color bar, scale, and a north arrow were incorporated into the final product.

2.3: Coastal Changes Maps

For this study, four satellite imagery data from Landsat 8, equipped with OLI/TIRS spectral bands, was utilized. The four satellite images downloaded are from July 21, 2019, January 13, 2020, January 18, 2022, and March 3, 2024. To ensure precision in our analysis a comprehensive examination over a five-year, leaving one year without analyzing for not making this monotonous. The data was sourced from the Earth Explorer website, a USGS platform facilitating access to a comprehensive catalog of satellite and aerial imagery. The data images downloaded from the satellite were first order, to start analyzing it from zero.

The data downloaded had minimal cloud cover; however, one of images, 2020, did exhibit cloud interference. To mitigate this, the ENVI software was employed to create our analysis and one of the first steps done was to remove clouds by the subsets in the preprocessing part of each image and remove excessive cloud coverage. The selection of the 2024 image

was particularly crucial to provide insight into the current state of the areas under investigation.

2.2.2: ENVI Software

Once all the images were downloaded, they were opened in ENVI Software for further processing. Prior to conducting any analysis, it was necessary to preprocess the images due to their original 30-meter spatial resolution, which was insufficient for the study, and the presence of stripping artifacts in all downloaded images.

To improve the spatial resolution of all satellite images from the different years, 2019-2024, the NNDiffuse Pan Sharpening tool was employed. This technique effectively increased the spatial resolution to 15 meters using the panchromatic band, enabling more detailed analysis. Subsequently, in order to address the presence of stripping, an atmospheric correction was performed using the dark subtraction tool. Following the atmospheric correction process, which eliminated the stripping effect, a subset of the imagery was utilized to refine the study area, specifically the Guayanilla coastline. This subset was selected to minimize cloud cover and enhance the clarity of the study site.

Once all preprocessing steps were completed, the analysis phase commenced. Utilizing the NDVI tool within ENVI Software, NDVI values were computed for each pixel in the imagery dataset. This facilitated the visualization of NDVI values representing vegetation density and health across the Earth's surface. The NDVI tool proved instrumental in providing valuable insights into vegetation distribution,

health, and temporal changes. Its capability to assign distinct numbers to vegetation based on NDVI values enabled the identification of vegetation presence or absence. This functionality rendered the NDVI tool indispensable for a multitude of applications, including agriculture, forestry, and environmental monitoring.

Following the calculation of NDVI, a mask was generated using the infrared band of the atmospheric corrected image. The threshold values for minimum and maximum varied across the different images analyzed. Once the mask was applied, Miss Perez Rivera was able to discern the temporal changes in vegetation with certainty. Remarkably, areas previously characterized by vegetation now showed signs of being inundated by ocean water, suggesting ongoing subsidence in these locations. This observation underscored the utility of the methodology in identifying and monitoring subsidence-related phenomena over time.

2.2.3 CARICOOS Buoy Data

To ascertain whether subsidence or sea level rise was predominantly affecting a specific portion of the south coast, the team consulted buoy data. The chosen buoy for analysis hailed from Magueyes Island in Lajas, Puerto Rico—[La Parguera MAPCO2 Buoy \(caricoos.org\)](https://caricoos.org). Observing the water level measurements with tide level data corresponding to the exact days of image analysis.

2.2.4 Meteorological Data

To determine whether the water flooding was caused by freshwater or saltwater intrusion due to ocean water

subsidence, they consulted meteorological data for each day from [NOAA - National Weather Service - Water](#). Since meteorological data is measured from 8 am of the day before to 8 am of the following day. The data examined was starting from the day after the selected image. For example, if the first analyzed image was from July 21, 2019, the meteorological data checked was from July 22 to ensure a complete view of the weather conditions from the day before. This thorough approach helped them understand the factors influencing the water conditions during the specified period.

III. Results and Discussion

3.1: Terrain Deformation

3.1.1: Displacement between July 8th and 20th, 2019

Upon analyzing the displacement map (**Figure 2**), it was discernible that greater subsidence, more negative displacement values, occurred toward the center of the island as opposed to the coastal area. In this case, there may be a problem with the C-band used in this study, given its classification as a lower or medium-penetration frequency band. Within forested regions, the dense vegetation cover impedes penetration, rendering the band ineffective in detecting changes in land elevation. Consequently, the C-band's sensitivity to vegetation movement in forested areas leads to misinterpretation, portraying such movement as subsidence (Fernández, L.A., n.d.). This phenomenon likely contributes to the observed higher subsidence values towards the center of the island. Nevertheless, it is important to

note that this limitation does not impact the study area, as it is situated in a region characterized by minimal vegetation or arid conditions. Such conditions facilitate the C-band's ability to effectively capture elevation changes within the study area.

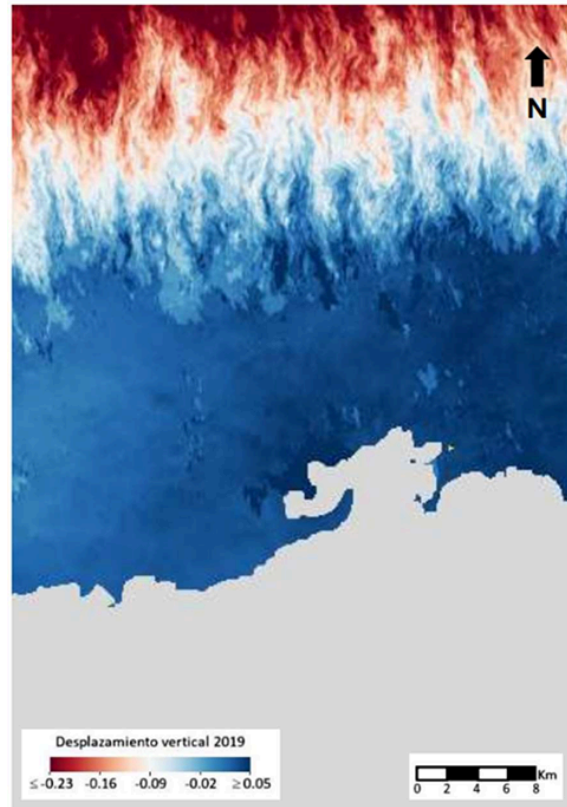


Figure 2: Observed displacement between July 8 to 20, 2019. During this time frame, the seismic sequence had not yet commenced.

3.1.2: Displacement between July 11th and 30th, 2023

An analysis of the displacement map (**Figure 3**) revealed distinct areas within southern Puerto Rico exhibiting both positive and negative (subsidence) values. The maximum reported subsidence within the depicted region amounted to 0.20m. In the town of Guayanilla, different regions displayed varying positive and negative values as well. The community of El Faro

experienced a reduction of 0.058m (~2.28in) in elevation. Given El Faro's characteristic as a coastal community with relatively flat terrain, this decline bears substantial implications for sea level dynamics. On the other hand, Punta Ventana Beach, situated near the epicenter of the largest earthquake of January 7, experienced a subsidence of 0.082m (3.22in), surpassing that of the El Faro's. The ongoing subsidence within this region has the potential to induce substantial alterations in its geomorphology, a phenomenon that will be further explored in the subsequent discussion.

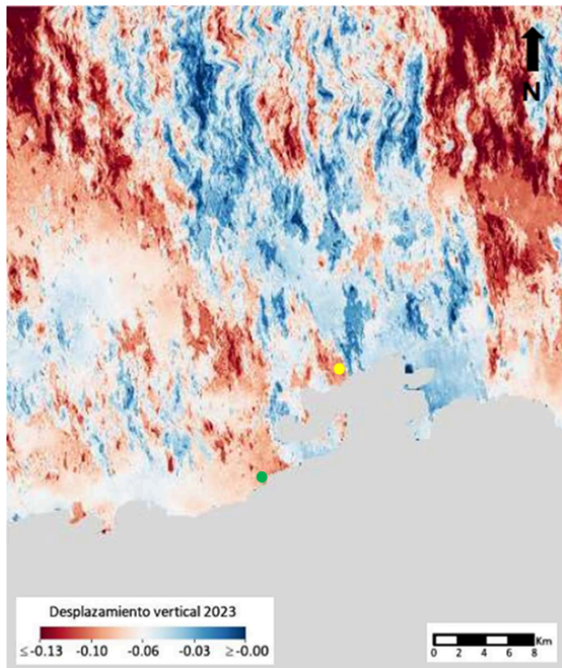


Figure 3: Observed displacement between July 11 to 30, 2023. The map illustrates the vertical displacement of the terrain three years after the 2020 seismic event. Study locations are marked by dots, with El Faro community indicated in yellow and the Punta Ventana Beach highlighted in green.

3.2: Coastal Changes Maps

3.2.1 Coastal Changes from 2019 to 2024

Through comprehensive analysis of coastal change maps, it becomes evident that land inundation caused by subsidence is progressively intensifying over time (**Figure 4**). By examining vegetation reflectance across near-infrared (NIR) and red bands, as proposed by Rouse et al. (1974), it was able to quantify solar energy absorption within the coastal wetland ecosystem in Guayanilla. In healthy vegetation, red coloration is prominent in the visible spectrum, leading to absorption of light in the red portions of the electromagnetic spectrum and reflection in the NIR range. The utilization of NDVI offers a valuable comparative measure for evaluating vegetation dynamics and temporal changes.

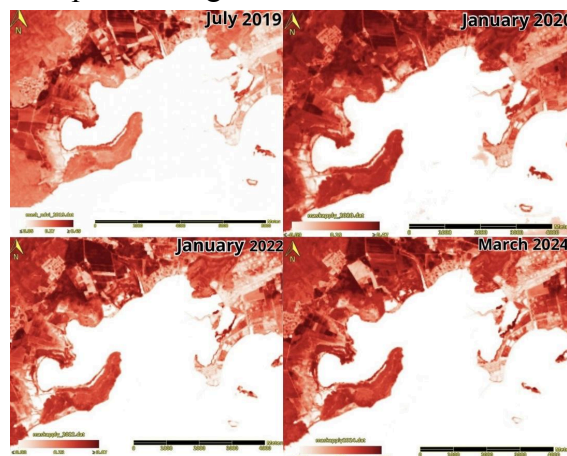


Figure 4: A sequence of images that show how the study area health of the vegetation had changed over time.

On July 21, 2019, the study area confronted an acute drought, as reported by DNA (2021). Consequently, the vegetation exhibited a pallid appearance, characterized by a spectral reflectance value of less than 0.27 (**Figure 5**). Notably, in the wetland areas of both

locations, vegetation persisted, displaying reflectance values exceeding 0.06. Despite the occurrence of scant rainfall during this period, amounting to less than 0.25 inches, its impact on vegetation dynamics is expected to be minimal (**Figure 6**).

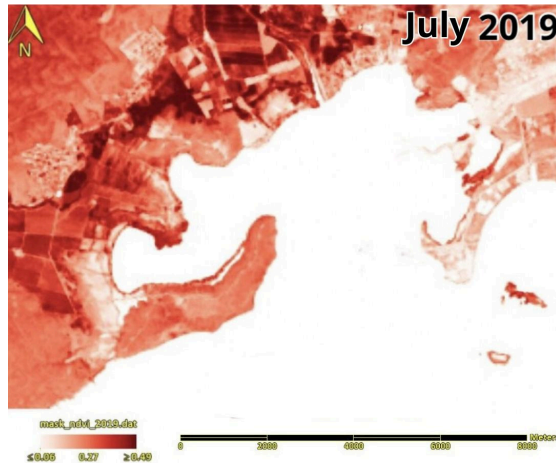


Figure 5: The Normalized Difference Vegetation Index (NDVI) calculation for the study area in July 2019.

January 13, 2020, six days after a 6.4 magnitude earthquake, reveals a complex interplay of environmental impacts. With 177 aftershocks recorded in close proximity to the study sites. Coastal change analysis revealed notable shifts in vegetation distribution, marked by increased presence with reflectance values exceeding 0.47 (**Figure 7**). However, concerning signs of degradation emerged in the wetland of Punta Ventana Beach, where vegetation appeared visibly lighter with reflectance values at least of 0.01. Furthermore, the intertidal lagoon in the community of El Faro exhibited synchronous reflectance patterns with ocean waters, with a value of 0, suggesting potential disruptions in ecological equilibrium (**Figure 8**).



Figure 6: Google Earth images show Punta Ventana Beach and the El Faro community in Guayanilla, Puerto Rico, taken in July 2019. Despite a severe drought, both areas were notably distanced from the ocean water by several meters, highlighting the impact of environmental changes on coastal regions.



Figure 7: The Normalized Difference Vegetation Index (NDVI) calculation for the study area in January 2020.



Figure 8: Google Earth images show Punta Ventana Beach and the El Faro community in Guayanilla, Puerto Rico, taken in January 2020. The community's El Faro image of ocean intrusion in the intertidal lagoon.

In the two-year span leading up to the coastal change map of January 18, 2022 (Figure 9), seismic activity in the southern region of Puerto Rico remained relatively subdued, with only six earthquakes registering at Mw 3 or less during that date. Nevertheless, a comparative analysis between this map and its 2020 counterpart reveals significant alterations, particularly evident in the wetland of Punta Ventana Beach, where vegetation presence has dramatically declined, with values approaching zero (Figure 10a). Similarly, the community of El Faro exhibits sparse vegetation in the intertidal lagoon (Figure 10b), while an adjacent wetland at east displays patches of ocean water with a

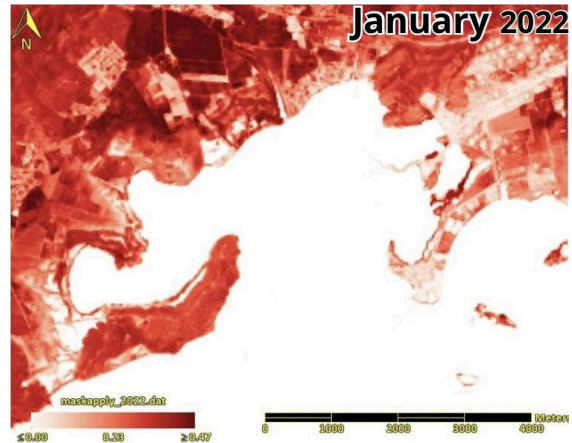


Figure 9: The Normalized Difference Vegetation Index (NDVI) calculation for the study area in January 2022.



Figure 10: Google Earth images show Punta Ventana Beach and the El Faro community in Guayanilla, Puerto Rico, taken in January 2022. Both study areas feature ocean water within the wetlands.

reflectance value of zero, further highlighting ecological shifts within the region.

In the course of the study year, 2024,

seismic activity persisted in the southern region of Puerto Rico. To ensure comprehensive analysis, an image from March 3, 2024, was analyzed to observe the area's evolution. Portions of Punta Ventana Beach, previously inundated with ocean water in January 2022, now exhibited approximately 0.25 vegetation reflectance (**Figure 11**). However, the swamp area behind and east of the beach remained flooded, with some sections registering reflectance values below -0.01 (**Figure 12a**). Contrastingly, El Faro community appeared more inundated compared to 2022, with the intertidal lagoon devoid of vegetation, now integrated into the ocean. Adjacent wetland to the east displayed patches of ocean water with -0.01 reflectance (**Figure 12b**). These annual alterations underscore a growing concern, as any storm tidal event could significantly impact both regions. Notably, Punta Ventana Beach, one of the study sites, has undergone the most pronounced changes over the past four years. If the seismic activity persists in the southern region of Puerto Rico, it could precipitate not just subsidence, but potentially geological shifts in the area.

3.2.2 CARICOOS Buoy Data

The analysis of tidal data from the Magueyes Island buoy in La Parguera, Lajas, Puerto Rico was crucial for understanding whether the increase in ocean water levels was related to the seismic sequence. By comparing tidal data between July 21, 2019 (**Figure 13**), and January 13, 2020 (**Figure 14**), it was observed that there was only a minimal increase in ocean water levels. In 2019, the maximum tide heights on both dates

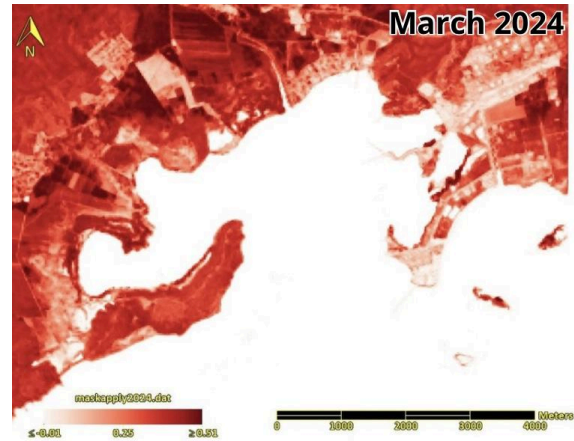


Figure 11: The Normalized Difference Vegetation Index (NDVI) calculation for the study area in March 2024.



Figure 12: Google Earth images show Punta Ventana Beach and the El Faro community in Guayanilla, Puerto Rico, taken in March 2024. Both study areas feature ocean water within the wetlands. The Punta Ventana Beach showing some plant growth in the inundated area.

were below 1 foot, whereas in 2020, they exceeded 1 foot, with a maximum tidal level of 1.13 feet recorded on January 13,

2020. However, these levels gradually decreased over time (Figure 15 and 16), indicating that the increase in ocean water levels was not attributable to the seismic sequence. Instead, this suggests that the rising ocean levels are more likely due to sea level rise rather than seismic activity (Figure 17).

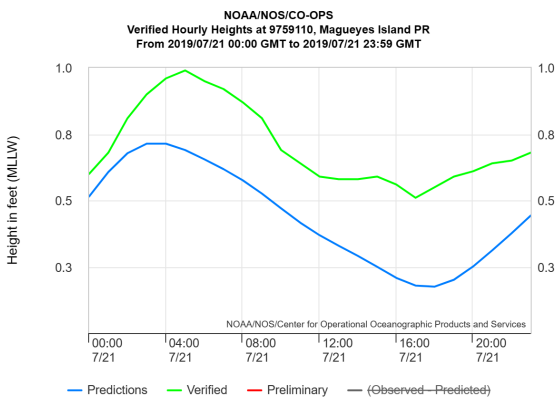


Figure 13: Tide gauge of Magueyes Island in Lajas, Puerto Rico from July 21, 2019. The high tide had a value of 0.99ft while the low tide reached to 0.51ft.

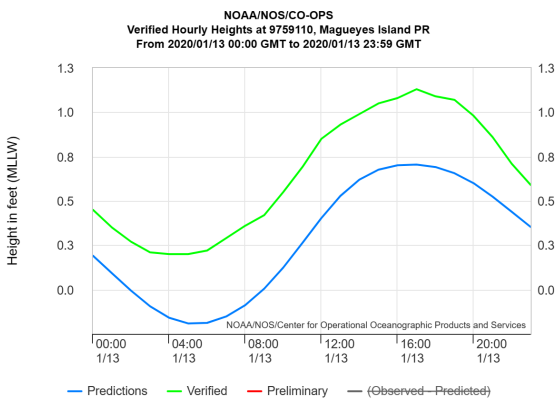


Figure 14: Tide gauge of Magueyes Island in Lajas, Puerto Rico from January 13, 2020. The high tide reached 1.13ft while the low tide was 0.22ft.

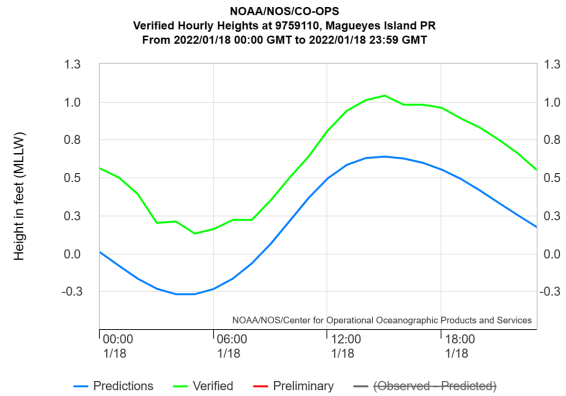


Figure 15: Tide gauge of Magueyes Island in Lajas, Puerto Rico from January 18, 2022. The high tide had a value of 1.04ft while the low tide reached to 0.13ft.

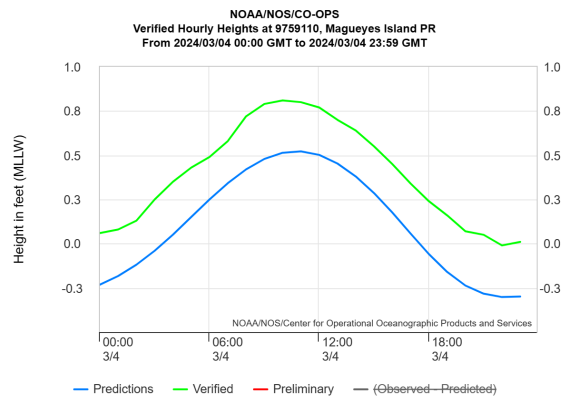


Figure 16: Tide gauge of Magueyes Island in Lajas, Puerto Rico from March 3, 2024. The high tide had a value of 0.78ft while the low tide reached -0.4ft.

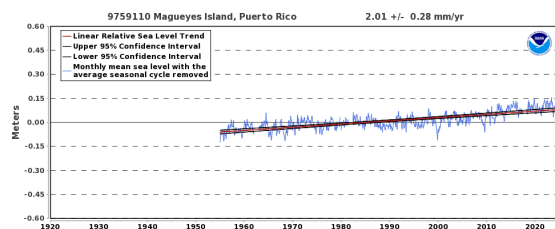


Figure 17: The sea level trend is influenced by climate change, whereas seismic activity has not shown such a dramatic increase.

3.2.3 Meteorological Data

The analysis of meteorological data was instrumental to assess the water conditions within the study areas of Punta Ventana Beach and El Faro community. Specifically, it helped determine whether the wetland was inundated by freshwater or ocean water. Reviewing meteorological records from July 21, 2019 (**Figure 19**), and March 3, 2024 (**Figure 20**), revealed precipitation levels of 0.01 to 0.10 inches in the study area. On January 13, 2020 (**Figure 21**) and January 18, 2022 (**Figure 22**) no precipitation had happened in the area. This data suggests that the water present in the wetland areas did not originate solely from precipitation. Instead, it confirms the increasing subsidence over the years (2020-2024) and indicates that the water in both locations is primarily composed of ocean water.

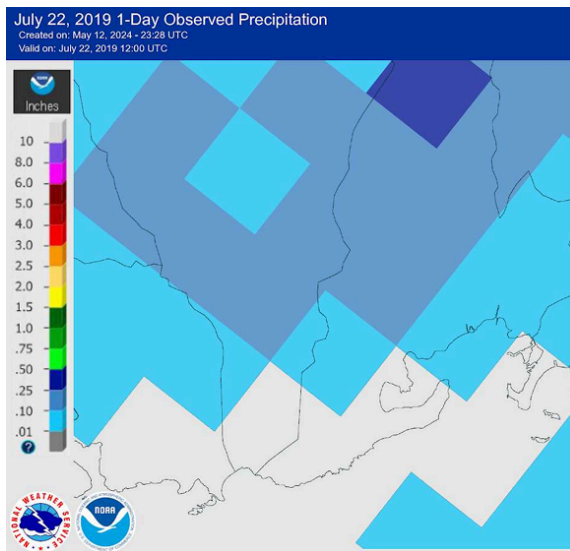


Figure 19: The precipitation magnitude in the study area on July 21, 2019, is chosen a day after because it represents the precipitation over the last 24 hours.

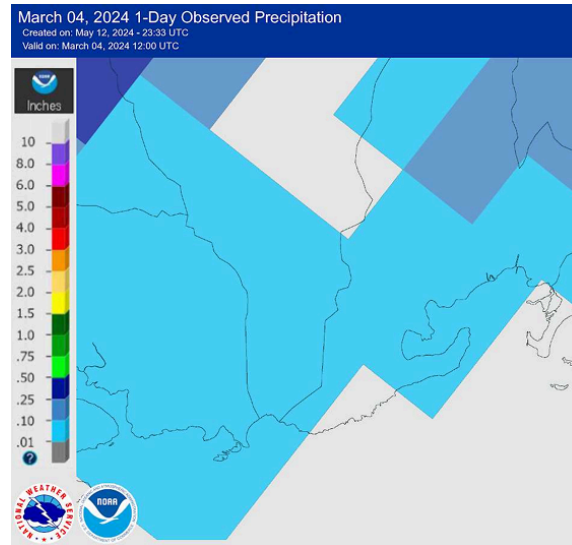


Figure 20: The precipitation magnitude in the study area on March 3, 2024, is chosen a day after because it represents the precipitation over the last 24 hours.

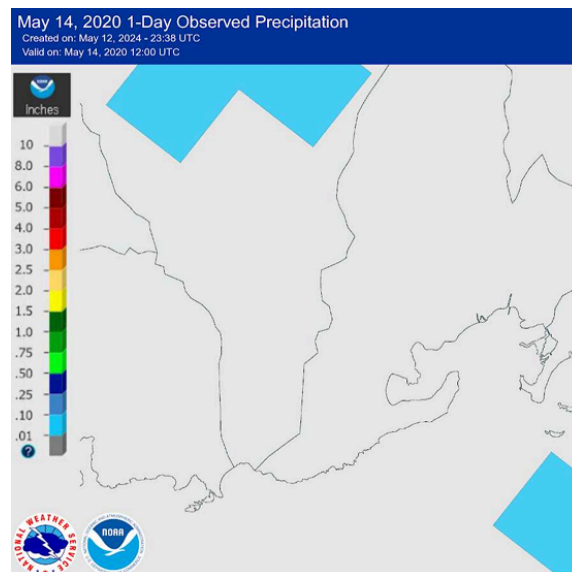


Figure 21: The absence of precipitation in the study area on January 13, 2020, prompts the selection of the following day to capture any precipitation that occurred within the last 24 hours.

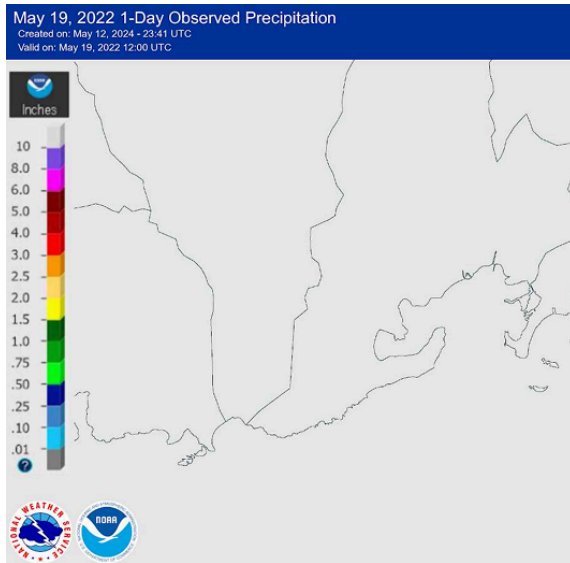


Figure 22: *The absence of precipitation in the study area on January 18, 2022, prompts the selection of the following day to capture any precipitation that occurred within the last 24 hours.*

IV. Conclusion

The seismic sequence of southern Puerto Rico, starting in December of 2019, caused the Mw 6.4 earthquake of January 7, 2020. The seismic activity aftershocks were very active in 2020 and still in 2024 they continue but less frequent, being one of the more active seismic sequences in the world and in our time (Lopez T.M, Castro, A.R, 2020). As a consequence of the seismic activity, there was a descent in elevation on the coastal areas. This decrease in elevation, measuring 0.058 m in El Faro community and 0.082 m in Punta Venta Beach, has led to intrusion of ocean water in the study area. Consequently, significant impacts have been observed, such as the integration of the intertidal lagoon into the ocean in El Faro community and increased flooding in Punta Ventana Beach could potentially lead to the fragmentation of the land and

the formation of a separate islet apart from the mainland. Additionally, subsidence in the area has been identified as a contributing factor to the entering of salty, oceanic water into these locations.

Continued flooding of these regions could lead to significant changes, highlighting the urgent need for comprehensive coastal management and adaptation strategies. Addressing the intricate challenges caused by subsidence and sea-level rise in coastal regions requires strategic interventions and collaborative efforts aimed at mitigating risks and improving resilience to future environmental threats.

V. Recommendations for future works

To effectively address the challenges posed by ground deformations, particularly in coastal regions like Punta Ventana Beach and the El Faro community in Guayanilla, continuous monitoring is paramount. This monitoring serves as a critical tool for assessing the risk of coastal flooding and identifying communities in need of potential reconstruction or relocation due to increased susceptibility to such inundation events. Vigilant analysis of these study sites is essential to gauge the evolving threats of coastal inundation and subsidence, especially considering their vulnerability to extreme events like storm tides or spring tides, making them more at risk compared to other coastal areas in Puerto Rico.

Furthermore, it is imperative to broaden the scope of study to encompass additional regions in southern Puerto Rico. Areas like Peñuelas and Ponce to the east, and Yauco, Guánica, Lajas, and Cabo Rojo to the west, warrant investigation to gain a

comprehensive understanding of the dynamics within the seismic zone. This expansion would facilitate the examination of coastal retreat patterns over time.

A crucial recommendation for relevant agencies is the deployment of measurement instruments, such as GPS devices, in these study areas to obtain more precise data for future studies on both vertical and horizontal displacements along faults in the southwest region of Puerto Rico. GPS technology, renowned for its accuracy in monitoring subsidence and land sinking over time, is pivotal in this regard. Continuous data provided by GPS instruments enables a deeper understanding of subsidence patterns and their underlying causes, thereby informing essential preventive or corrective measures. By utilizing GPS technology, a comprehensive analysis of fault movements and displacements resulting from seismic events can be conducted (Hofmann-Wellenhof, B., 1992).

Lastly, community education is paramount, particularly for residents of the El Faro community. It is crucial to inform them of the realities surrounding their environment and the risks they face. It is advisable for someone from the community to guide them through the situation and the potential need for relocation. For those unable to afford relocation, it is essential to provide assistance, ensuring their transition to a safer location with all expenses covered. By prioritizing education and support, communities can make informed decisions and take necessary actions to safeguard their well-being in the face of environmental challenges.

VI. References

1. Barreto-Orta, M., Mendez-Tejada, R., Rodriguez, E., Cabrera, N., Diaz, E., & Perez, K., 2019, State of the beaches in Puerto Rico after Hurricane Maria (2017): *Shore &*, v. 87(1), p. 16–23.
2. Barreto, M. 2017, Assessment of Beach Morphology at Puerto Rico Island. Reporte técnico DRNA y NOAA. 58.
3. Fernández, L.A., n.d, SAR Synthetic-Aperture Radar: Detektia, accessed in April 2024.
4. Hofmann-Wellenhof, B., Lichtenegger, H., and Collins, J., 1992, *Global Positioning System*: Vienna, Springer Vienna.
5. Internet Geography, 2023, How do geological structure and rock type influence coastal landforms (accessed May 2024).
6. López Marrero, T., Castro Rivera, A. 2020. A seis meses del 6.4. Centro Interdisciplinario de Estudios del Litoral. Mayagüez, PR: Universidad de Puerto Rico. 6 p.
7. NOAA, 2021, What is a barrier island?: [What is a barrier island? \(noaa.gov\)](https://www.noaa.gov/what-is-a-barrier-island/) (accessed May 2024).
8. [Puerto Rico Seismic Network \(uprm.edu\)](https://www.uprm.edu/seismic-network/)
9. Ten, Brink, U.S, Vanacore, E.A., Fieldings, E.J., Chaytor, J.D., López-Venegas, A.M., Baldwin, W.E., Foster, D.S., and Andrews, B.D., 2022, Mature Diffuse Tectonic Block Boundary Revealed by the 2020 Southwestern Puerto Rico, Seismic Sequence: *Tectonics*, v. 41, p. 1-18.

10. Terremotos en Puerto Rico - Eco Exploratorio: Museo de ciencias de Puerto Rico, 2022, EcoExploratorio: Museo de Ciencias de Puerto Rico, <https://ecoexploratorio.org/a/menazas-naturales/terremotos/terremotos-en-puerto-rico/> (accessed May 2024).
11. Sentinel-1 - Sentinel Online (copernicus.eu) (accessed April 2024).
12. Shirzaei, M., Freymueller, J.T., and Minderhoud, P., 2021, Measuring, modeling, and projecting coastal land subsidence: Nature Reviews Earth & Environment, v. 2, p. 40-58.
13. Styron, R., 2019, Coseismic uplift and subsidence: An underappreciated seismic threat: GEM Hazard (accessed May 2024).
14. U.S. Geological Survey, Landsat 8: [Landsat 8 | U.S. Geological Survey \(usgs.gov\)](#) (accessed May 2024).
15. U.S. Geological Survey, NOAA Ocean Exploration and Research, Imagery created with geomapapp (accessed March 2024).
16. Tides, N., and Currents NOAA tides and currents: Noaa.gov, <https://tidesandcurrents.noaa.gov/> (accessed May 2024).
17. [Informe sobre los eventos de Sequía de 2018-2020 en Puerto Rico \(pr.gov\)](#)